ACS APPLIED MATERIALS & INTERFACES

Research Article

www.acsami.org

Time-Dependent Scattering of Ultrathin Gold Film under Potential Perturbation

Yu Huang,* Mark C Pitter, and Michael G Somekh

IBIOS, Department of Electrical and Electronic Engineering, University of Nottingham, NG7 2RD, United Kingdom

ABSTRACT: Shifts of the plasmon scattering band of ultrathin gold films under the effect of dynamic applied potential were studied in single wavelength measurements. The effect on scattering of applied potential was ascribed to electronic charging and discharging of the gold film. Scattering transients in response to square-wave potential modulation had an exponential form which depended on the potential step width, the modulation frequency and the nature of the ions. The presence of an AC signal component induced by ±10 mV potential modulated at 2 kHz indicated the capability of very thin gold film to respond to high frequency voltage.

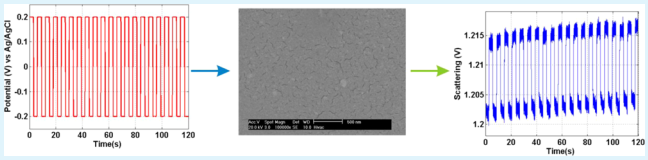

KEYWORDS: *ultrathin gold film, plasmon scattering, potential step transient, optical biosensor*

1. INTRODUCTION

The optical properties of ultrathin noble metal films evaporated on transparent substrates have been widely studied due to their potential applications in chemical and biological sensing.[1,2] The nanosized structures distributed on the substrate exhibit the phenomenon of localized surface plasmon resonance (LSPR), which is similar to the plasmon resonance that arises from dispersed metal nanoparticles. The resonance frequency of LSPR is highly dependent on the particle size, shape and the dielectric constant of both the particle and its surrounding medium, since all of these factors have an effect on the electron density at the particle surface.[3,4] The change in the particle's electron density can be directly regulated by an applied potential, which results in the presence of a double layer capacitance on the particle surface. Charges stored in the double layer capacitor adjust the conduction electron density, which in turn leads to the alteration of its plasma frequency and a shift in its plasmon absorption or scattering band.[5−9]

Optical recording of neural activity using a gold nanoparticle array has been previously reported.[10] The shift in the plasmon resonance was caused by electron transport within the noble metal induced by the cellular action potential. The success of this noninvasive optical method encourages the study of nanoparticle in vitro and in vivo application to measure neural activity because it overcomes the drawbacks of photobleaching and phototoxicity inherent in the use of voltage sensitive fluorescent dyes. A systematic exploration of the potential-dependent optical properties of nanostructure is essential to understand their relationship. We have recently measured the morphology dependent voltage sensitivities of Au nanospheres, nanorods, nanoprisms and thin films and found that 16 nm ultrathin gold film exhibited the highest voltage sensitivity due to a very large surface area to volume ratio and stronger plasmonic coupling of overlapped nanostructures.[11] The challenges of the application of recording neural activity on the basis of noble metal nanostructure arise from the small and fast cellular electrical signal. A comparably short response time and large spectral change are desirable, because this will determine the sensitivity and quantification of the plasmonic change.

Here, we report our studies on the response of 16 nm ultrathin gold film to dynamical potential. The monitoring of the plasmon scattering band of ultrathin Au film using dark-field spectroscopy is a relatively convenient technique to study the potential-dependent optical properties of noble metal nanostructure, as compared to the electrochemical surface plasmon resonance technique, which is often implemented using the Kretschmann-Raether configuration.[12−15] The shift in scattering of ultrathin Au film is modulated by non-Faradic potential so that the interference of redox active species was excluded from this study. The potential dependent scattering transient has a relationship with the effect of ions on the formation of the double layer. A detectable signal produced by a potential of ±10 mV at 2000 Hz would open up the possibility of using noble metal nanostructure-based sensors in monitoring the neural activity in real time.

2. EXPERIMENTAL SECTION

Ultrathin Gold Film Preparation. Ultrathin gold film was prepared on glass substrates with a thermal evaporation system equipped with an Edwards FTM-5 film thickness monitor. Gold wire (99.99% purity, Advent Research Materials Ltd.) was heated up to be gold atoms at the beginning. Gold atoms have sufficient thermal energy to diffuse on the bare substrate as clusters and prefer to initially grow on the glass substrate surface in a lateral direction. As evaporation continued, these gold clusters get in close contact with each other to increase the coarseness of metal surface. The vertical layer growth commenced after gold clusters fully coalesced on the substrate surface.[16] Evaporation was performed under high vacuum of

Received: March 9, 2012
Accepted: July 18, 2012
Published: July 18, 2012

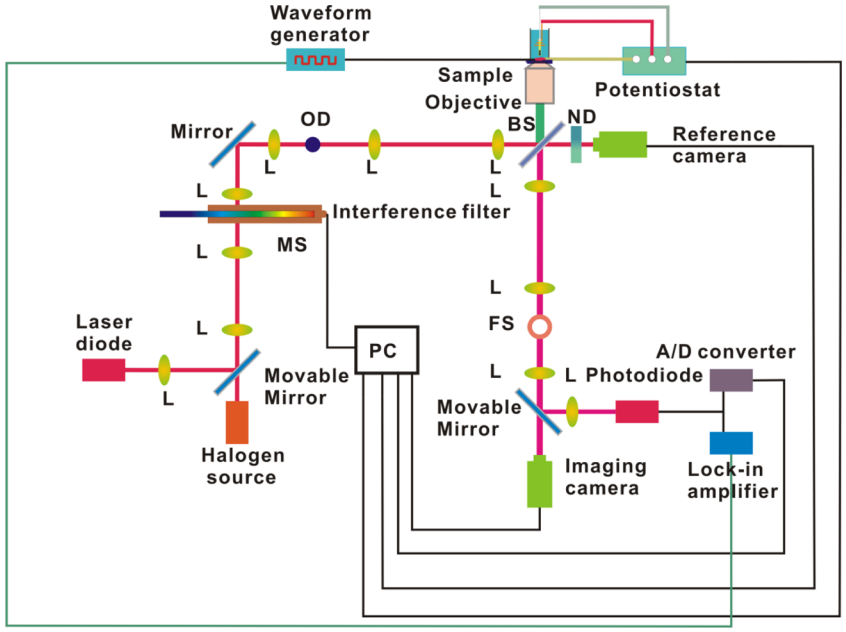

Figure 1. Schematic of the dark-field imaging spectrometer configuration. L, achromatic lens; BS, pellicle beamsplitter; ND, neutral density filter; MS, motorized stage; OD, opaque disk; FS, field stop.

pressure ~2 × 10^{-6} Torr and a deposition rate of 0.1−1.5 nm/s. The film thickness of ~16 nm was determined using a Rank Taylor Hobson Talystep surface profilometer.

Spectroelectrochemical Measurement. An electrochemical cell was designed in-house to permit modulation of electron density of the gold film (working electrode) which was illuminated by reflected light. The counter electrode (coiled Au wire) and reference electrode (Agl AgCllsaturated NaCl) were configured above the working electrode. A potentiostat (VersaSTAT 3, Princeton Applied Research) was used to control the potential of the working electrode. The base electrolyte solution used in the electrochemical measurement was 0.1 M NaCl. All the potentials were cited with respect to this reference electrode unless stated.

The scattered light from the gold film was studied by a custom-built, reflected light, dark-field inverted microscope, and its schematic is shown in Figure 1. The angle of incident light was designed at 44°.[11] The wavelengths of unpolarized white light from a halogen lamp were selected by a linear variable interference filter (VIS-NIR 200, Edmund Optics) and two CCD cameras (SXVF-M7, Starlight Xpress) were performed as imaging and reference sensors respectively. The imaging camera recorded the light scattered by gold film and the reference camera monitored the light intensity stability at each wavelength in order to minimize the effect of any fluctuations in the light source.

For dynamic measurements, an integrated photodiode and amplifier (PDA100A-EC, Thorlabs) served to detect the light scattered by the gold film. A laser diode (635 nm, CPS180, Thorlabs) was used as the illumination source with a collection spot size of about 15 μm at the sample surface. The signal collected by the photodiode was monitored by an analogue-to-digital converter (PCI-DAS1602/16, Measurement Computing). The time resolution was 0.2 ms.

When a high frequency potential provided by a waveform generator (33220A, Agilent Technologies) was applied on the gold film, the signal from the photodiode was fed into a lock-in amplifier (SR850, Stanford research systems) to extract the high frequency signal I_{ac} of the scattered light modulated by the ac potential. Simultaneously, the signal collected by the photodiode was time-averaged to obtain the dc intensity, I_{dc}. The ac component normalized by the dc, (I_{ac}/ I_{dc}), represents the degree response of the gold film to ac potential relative to the background of scattered light.

3. RESULTS AND DISCUSSION

The scattering spectrum of this gold film immersed in 0.1 M NaCl measured by the dark-field spectrometer is shown in Figure 2. The spectrum increased monotonically with wavelength from the visible to the near-infrared region.

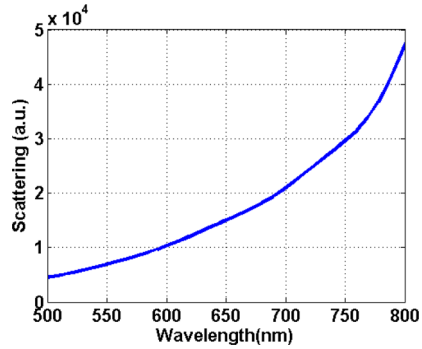

Figure 2. Spectrum of 16 nm gold film exposed to 0.1 M NaCl.

Cyclic voltammetry (CV) was used to determine the potential range in which the redox reaction was taking place on the gold film. Within the −0.6 to 1 V potential window (Figure 3a), the gold film experienced an oxidation peak at 0.4 V due to the formation of hydrated AuOH and AuO in the positive-going potential scan[15]

$$Au + 2H_2O \rightarrow AuOH{\cdot}H_2O + H^+ + e^- \quad (1a)$$

$$AuOH \rightarrow AuO + H^+ + e^- \quad (1b)$$

Potential greater than 0.8 V activated oxygen evolution. The reduction peak at 0.6 V during the cathodic potential scan arose from the reverse reaction of the above-mentioned process. At a potential lower than −0.4 V, the hydrogen evolution reaction began. The Faradaic reactions can be essentially eliminated by limiting the potential window. The approximately rectangular loop of the CV plot in Figure 3b indicated there was no Faradic

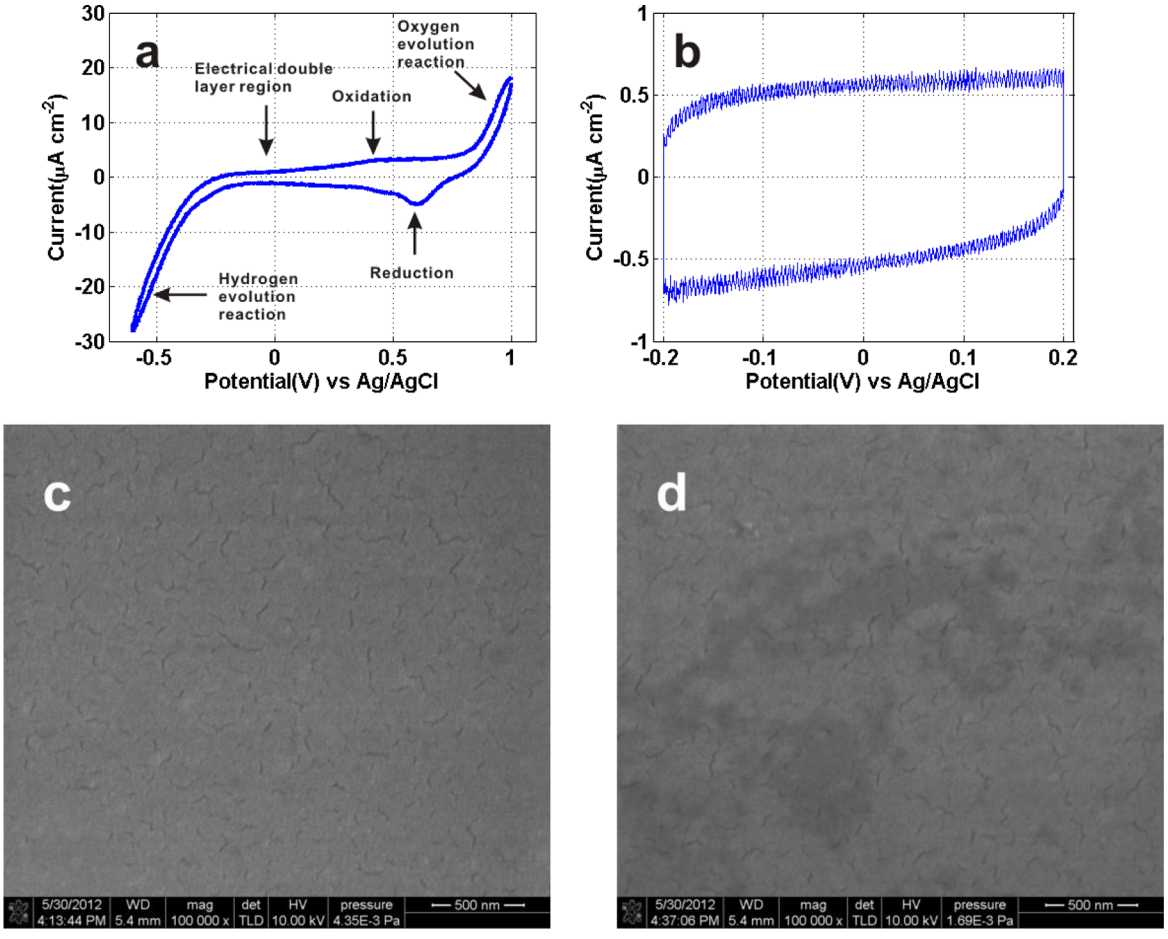

Figure 3. Cyclic voltammograms (CVs) of 16 nm Au film in 0.1 M NaCl with a potential scan rate 0.05 V/s. The oxidation peak and the reduction peak can be observed in (a). The CV curve of (b) indicates that potentials between ±250 mV are in the electrical double layer region for the gold film. The potential was applied vs Ag/AgCl. SEM images of 16 nm Au film on glass substrate (c) before and (d) after the application of ±250 mV.

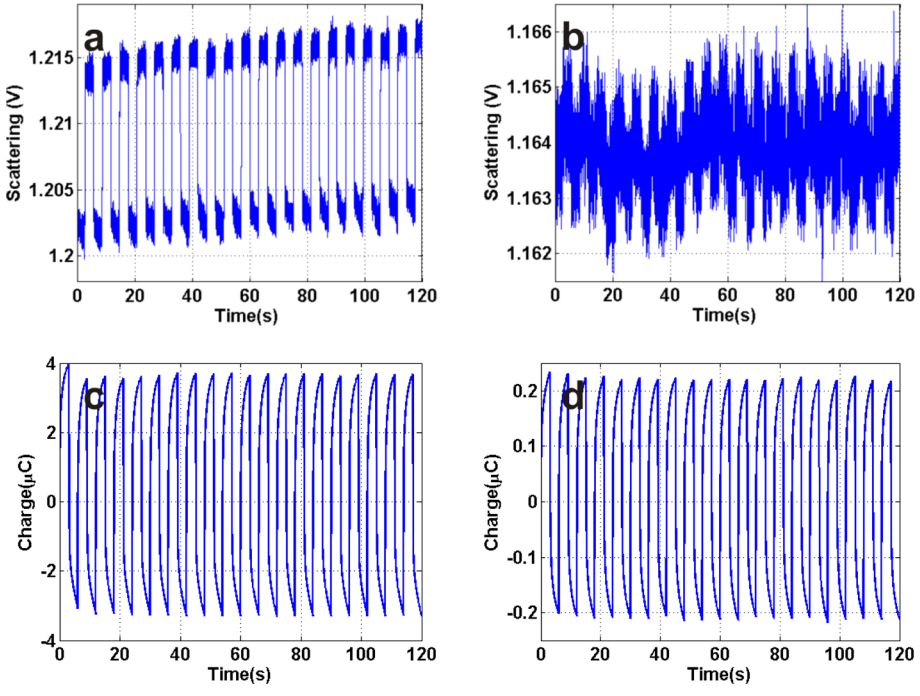

Figure 4. Scattering modulated by a square wave of (a) ±200 mV and (b) ±25 mV over a period of 6 s. Measurements of charge in response to the modulated potential of (c) ±200 mV and (d) ±25 mV.

dx.doi.org/10.1021/am301231m | ACS Appl. Mater. Interfaces 2012, 4, 3829−3836

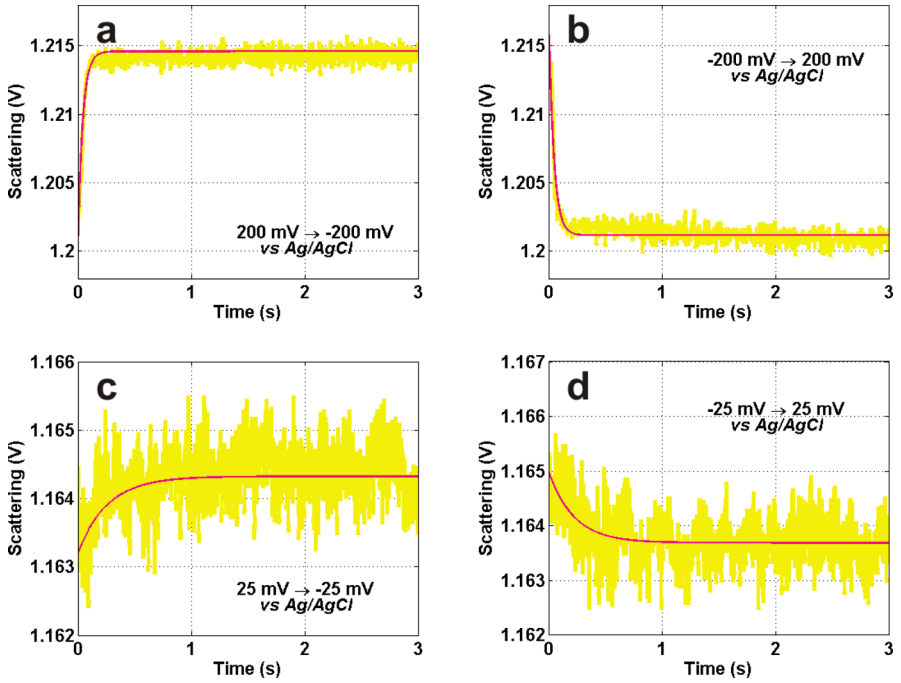

Figure 5. Change of scattering in response to a potential step from (a) 200 mV to −200 mV, (b) −200 mV to 200 mV, (c) 25 mV to −25 mV, and (d) −25 mV to 25 mV. The purple lines in a−d represent the fitted curve for eq 2.

process between ±250 mV. The observed current here was due to the movement of charges taking place in the electrical double layer, resulting in current displacement. The interference of redox reaction involved in the measurement can be avoided by limiting the potential applied to the Au film between 250 mV and −250 mV. SEM images of gold film before and after the application of ±250 mV are shown in panels c and d in Figure 3, respectively. The gold film surface is composed of large and interconnected gold structures. These elongated regions link up to form a percolating network, separated by short channels and crevasses.[16,17] Comparing the SEM images of gold film shown in panels c and d in Figure 3, its surface morphology has no significant change after the gold film was exposed to potential.

The voltage sensitivity of ultrathin gold film had previously been measured by using CCD cameras.[11] Although the use of spatial integration on the CCD chip can improve the speed of CCD cameras, it is still far from the millisecond time resolution necessary for observing the initial and crucial segment of the scattering transient perturbed by the potential. To circumvent this limitation, a photodiode was used as a sensor to detect the scattered light. A laser beam was chosen as the illumination source because it provides abundant optical power and the wavelength of 635 nm was located in the gold film's spectral window of high voltage sensitivity.

The transient scattering of gold film in response to square waves of ±200 mV and ±25 mV are shown in panels a and b in Figure 4. The scattering was switched by reversing the potential from positive to negative or from negative to positive and it changed with the potential. Simultaneous measurements of charge in response to potentials switched between ±200 mV and ±25 mV are shown in panels c and d in Figure 4. The charge was calculated as the time integrated total current. Coinstantaneous transients of scattering and charge were synchronized with the potential. The plot of charge was similar to that of the corresponding scattering (with a change in sign). The similar traits of scattering and charge was interpreted as that both are the product of potential. The charge associated with the current is the outcome of the charging-discharging process of the electrical double layer at the surface of the gold. Although the charge is almost in line with the scattering, the plateau of charge is not observable as the scattering does. This may be originated either from double layer charging process at the surfaces of gold or the slow electron exchanged between gold surface and adsorbed ion.[18]

The transients at each potential step can be fitted to the equation

$$I_{\text{scattering}} = a(1 - e^{-(t/\tau)}) + b \qquad (2)$$

where a is the change in scattering between the beginning of potential step b and the final steady-state, τ is the time constant and t is the time. Four examples of the fitted curves are shown in Figures 5a − 5d as purple lines and the values of (a, b, τ) were (0.0146, 1.2, 0.04288 s) for (200 mV → −200 mV), (−0.01584, 1.217, 0.04539 s) for (−200 mV → 200 mV), (0.001121, 1.1632, 0.2615 s) for (25 mV → −25 mV) and (−0.001311, 1.165, 0.2215 s) for (−25 mV → 25 mV) respectively. The ratio of $a/(a + 2b)$ representing the scattering contrast, the fractional content of change in scattering a relative to the sum of scattering strength before (b) and after the potential step ($a + b$), and the time constant τ, are dependent on the potential step width. The decrease in the potential results in the reduced scattering contrast and increased time constants.

The values of $a/(a + 2b)$ and τ produced by a series of 6 s period square wave potential modulation modes are shown in Figure 6. Although sample-to-sample variability will cause $a/(a + 2b)$ and τ have different values, the following tendency was always observed: (i) the absolute value of $a/(a+2b)$ in a positive potential step ($-E \rightarrow E$, $0 \rightarrow E$, $-E \rightarrow 0$) was almost equal to that in the corresponding negative potential step ($E \rightarrow -E$, $E \rightarrow 0$, $0 \rightarrow -E$), (ii) the absolute value of $a/(a + 2b)$ produced by potential changed between positive and zero ($E \rightleftharpoons$

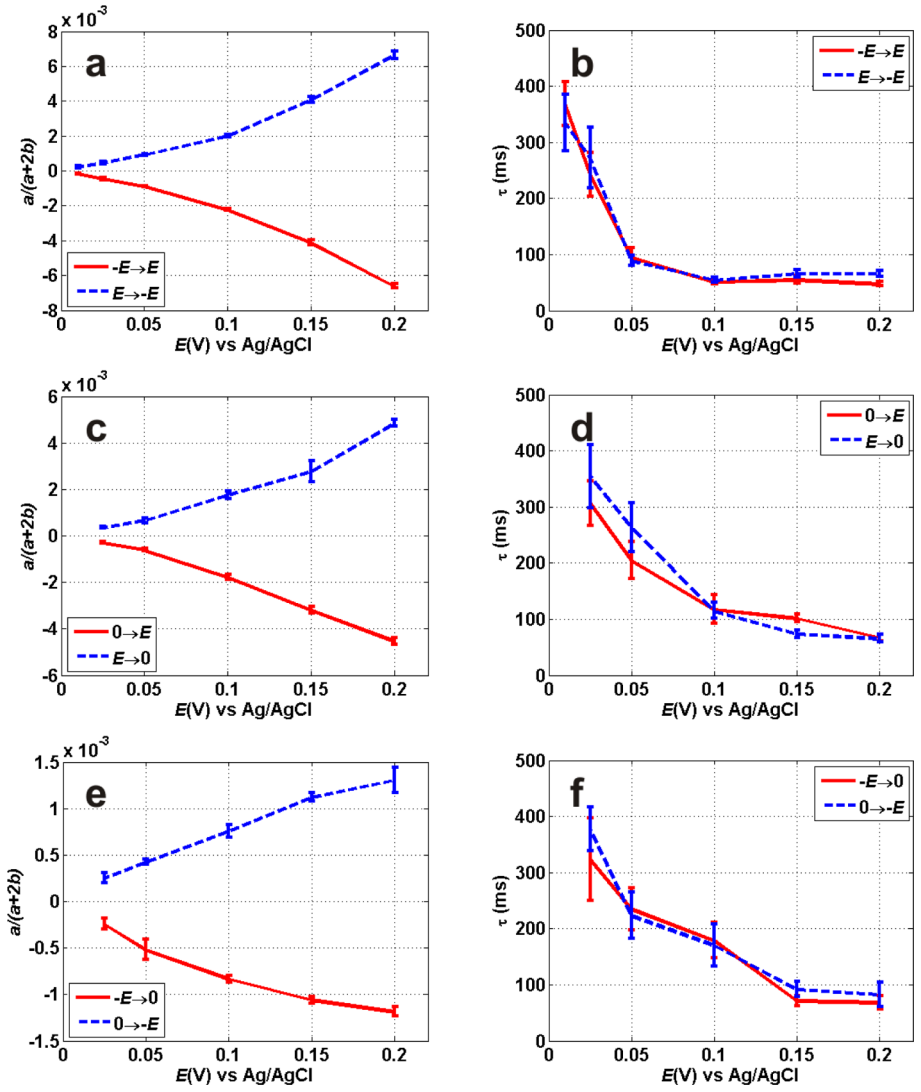

Figure 6. Scattering contrast $a/(a + 2b)$ conducted by potential step (a) $E \rightleftharpoons -E$, (c) $E \rightleftharpoons 0$, and (e) $-E \rightleftharpoons 0$. Time constant τ conducted by potential step (b) $E \rightleftharpoons -E$, (d) $E \rightleftharpoons 0$, and (f) $-E \rightleftharpoons 0$.

0) is larger than that produced by the corresponding potential changed between negative and zero ($-E \rightleftharpoons 0$), and (iii) the time constant τ increases with decreasing potential.

Anion Cl^- moves toward and cation Na^+ leaves the gold surface when the potential was stepped in the positive direction and their motions are reversed when the potential was stepped in the opposite direction. As may be expected with the same amount of charge exchanging on the gold surface modulated by positive and negative potential steps, with just reversed initial and final potentials, their scattering contrast illustrated in panels a, c, and e in Figure 6 is symmetrical with respect to the zero line.

Panels c and e in Figure 6 show the scattering contrast induced by the potential steps with initial and final potentials exchanging between positive and 0 V, and negative and 0 V, respectively. At this very low frequency of 1/6 Hz, adsorption capacitance and resistance would present in the potential range of double layer behavior[19] shown in Figure 3b. The anion Cl^- is expected to adsorb more strongly on the gold surface when the initial or final potential is positive, compared to the degree of cation Na^+ adsorbing on the same gold surface area in the case of negative potential. An adsorption capacitance C_{ad} created by the specific adsorption of Cl^- in parallel with the double layer capacitance C_{dl} of pure capacitive electrode dramatically increases the gold-electrolyte interfacial capacitance and the amount of electrons transferred in the gold.[20,21] As a result, an initial or final potential more positive than 0 V induces greater change in scattering than the effect of initial or final potentials less than 0 V applied to the gold surface, which can be seen from the larger value of $a/(a + 2b)$ in Figure 6c than that in 6e. Examining panels a and c in Figure 6, although the potential step in Figure 6c only experienced half cycle of that in Figure 6a, the high proportion of scattering contrast in Figure 6c to the scattering contrast in Figure 6a and their similar shape underline the contribution of Cl^- to the interfacial capacitance and the consequent change in scattering perturbed by potential.

The time constant τ is likely to be a product of the interfacial capacitance C_i and interfacial resistance R_i ($\tau = R_iC_i$). Cl^- strongly prefers to adsorb on the significant number of terraces and steps of gold surface than other ions in solvent, such as OH^-, at potential more positive than 0 V. The presence of specific adsorption of Cl^- at the gold/solution interface is potential dependent, which leads the magnitude of adsorption capacitance and adsorption resistance to be changed with

potential. Charge transferred between chloride anions and gold surface took place by this structure. Therefore, adsorption capacitance and resistance contributed significantly to the performance of gold film's potential dependent scattering. Once the gold surface is covered by adsorbed Cl^-, the interfacial capacitance is increased significantly, which has been illustrated by using the scattering contrast as a comparison in panels c and e in Figure 6. However, the value of time constant produced by large capacitance (Figure 6d) does not have too much difference as compared to the small capacitance case (Figure 6f). Taking into the account 0.1 M NaCl and frequency of 1/6 Hz potential used in this system, mass-transport limitations are negligible and partial charge transfer occurs during this process.[19] More anions were incorporated in the inner layer and adsorbed at the gold-electrolyte rough interface. As the fractional surface coverage of anion increases, the adsorption capacitance increases while the adsorption resistance correspondingly decreases. The value of adsorption capacitance and adsorption resistance changed in the opposite way, which is shown in Figure 7. The impedance spectra for

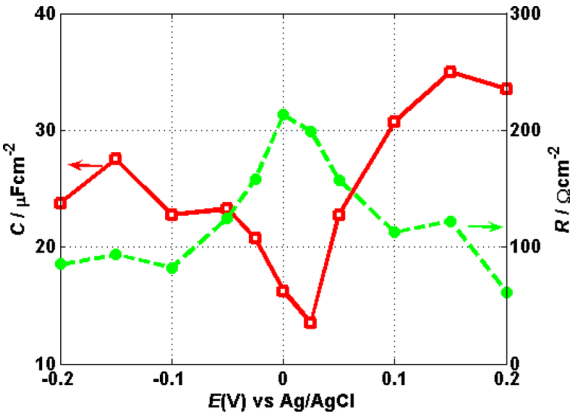

Figure 7. Plot of capacitance and resistance as a function of potential.

this potential region can be fitted by the equivalent circuits in refs 19, 20. When the magnitude of potential decreased, the adsorption capacitance decreases but the adsorption resistance increases. Therefore, the time constants produced by the potential step with potential changed between positive and zero $(E \rightleftharpoons 0)$ in Figure 6d and potential changed between negative and zero $(-E \rightleftharpoons 0)$ in Figure 6f are nearly the same no matter what are the polarities of initial and final potentials. Considering the effect of fractal character of the gold surface, the time constants in the case of full potential step range shown in Figure 6b have a similar value and trend as a function of potential in the case of half potential step range in panels d and f in Figure 6. The results of scattering contrast and time constant indicate that the nature of ions and fractal surface are important factors to determine the gold-electrolyte interfacial capacity. The larger capacitance at their interface does not need to consume longer time for charging.

The scattering transient perturbed by fast potential pulse is shown in Figure 8a–d. The scattered light follows the potential trace to move. With the increase in the potential frequency from 0.5 to 20 Hz, the characteristic exponential transient induced by the potential step gradually disappeared and the magnitude of scattering change was also reduced. The dependence of $a/(a+2b)$ and time constant τ on the potential frequency in the range of 1/6 to 20 Hz are shown in panels e and f in Figure 8. Both of them decayed with increasing frequency. When the potential is altered more and more rapidly, frequent exchange of cations and anions on the gold surface reduces the sustainability of the double layer. The time for counterions to develop the complete double layer becomes shorter and shorter. Although no Faradaic reaction took place in the potential range of ±50 mV, the double-layer adsorption capacitance on the rough gold surface is frequency dependent. The interfacial capacitance and resistance gradually decline with increasing frequency due to the presence of less adsorption ions on gold surface.[20,21] The capacitance dispersion represented by the trend of time constant was observed in Figure 8f.[19,22] The degree of modulation in the electron density is attenuated by the reduced capacitance and limited charging time. As a result, smaller scattering contrast and time constants are exhibited in the high frequency region.

A question is raised: "can 16 nm Au film respond to ac potential?" because its change in scattering decreases with increasing potential frequency. The answer to this question will determine the feasibility of using gold film, or even gold nanostructure, to monitor neural action potential. The capability of Au film to respond to 20 Hz square wave potential with a magnitude of ±50 mV has been demonstrated in Figure 8d. However, the ac component of the scattered light modulated by higher frequency potential is submerged in the noise and is undistinguishable. However, the sensitivity of lock-in amplification permits us to measure the ac component of scattered light in response to square wave potential from 1 Hz up to 2,000 Hz. The frequency dependent I_{ac}/I_{dc} shown in Figure 9 definitely gives a positive answer to this question. Although ±10 mV_{pp} was applied on the gold film with frequency up to 2000 Hz, the value of I_{ac}/I_{dc} still remain above 2×10^{-5}. This signal level reveals that the 16 nm Au film can response to high frequency potential. More importantly, while the real time detection of the scattered light perturbed by high frequency potential is beyond the resolution of our current optical system, the results suggest that by taking advantage of tunable surface plasmon resonance and advancement of electronic design, it might be possible to fabricate nanoparticle with specific size and shape suited to neural activity recording in the future.

4. CONCLUSION

The potential induced plasmon scattering of 16 nm Au film has been studied in detail. The potential width was restricted between ±250 mV to avoid the occurrence of redox reaction to interfere the measurement. The alteration in scattered light intensity synchronized with the change of Au film charge supported the fact that the modulation of scattering is mainly due to the charging-discharging process of Au film. The transient scattering in response to the potential step was characterized as an exponential form. The scattering contrast and the time constant derived from the exponential scattering transient curve were found to depend on the potential step width, potential frequency and the nature of the ions. The adsorption of Cl^- dramatically enhances the capacitance of gold film and the change in scattering, but the corresponding time constant is as small as the RC charging time in the case of the double layer mainly composed of Na^+. The decrease in potential results in the decreased capacitance and increased resistance at gold-electrolyte interface. Correspondingly, this reduced the change in scattering and increased the time constant. The increase in the potential frequency decreases the

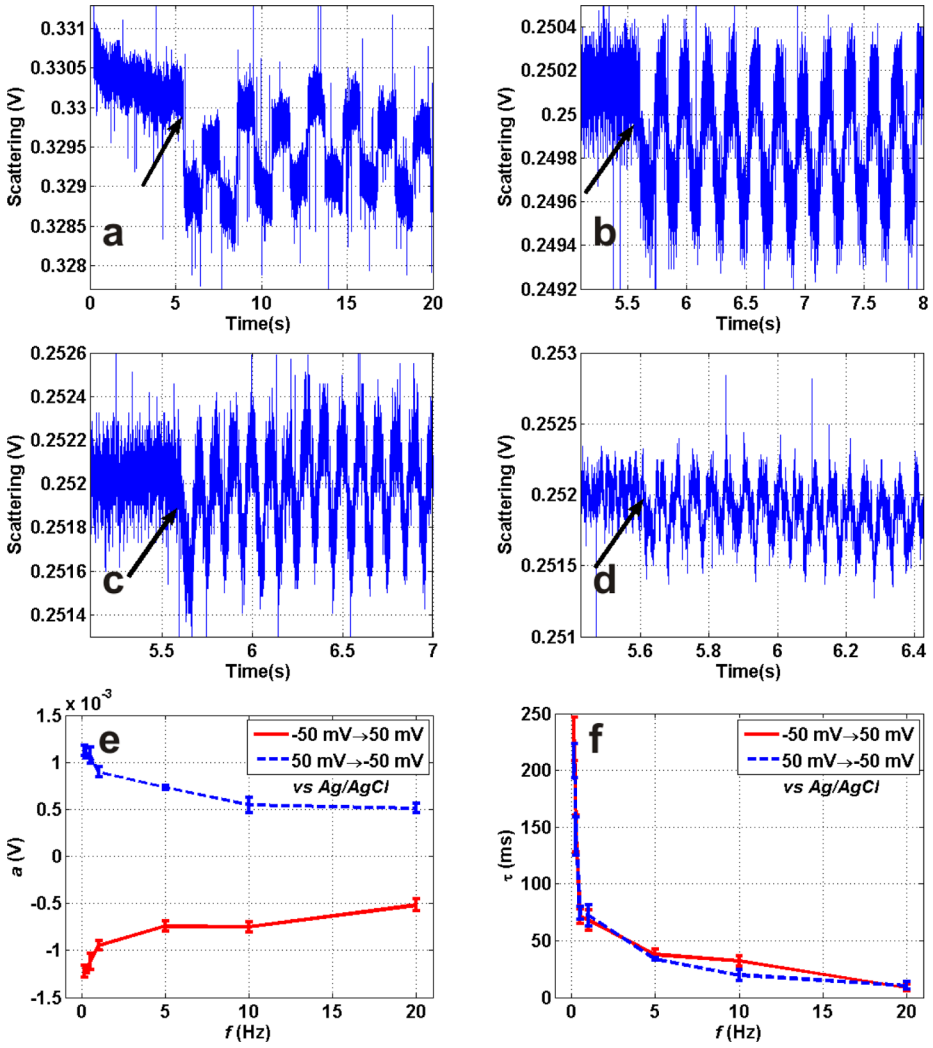

Figure 8. Scattering modulated by a square wave of ±50 mV vs Ag/AgCl with a frequency of (a) 0.5, (b) 5, (c) 10, and (d) 20 Hz. The arrows indicate the beginning of voltage application. Potential frequency dependence of (e) scattering contrast $a/(a + 2b)$ and (f) time constant τ in response to the square wave of ±50 mV.

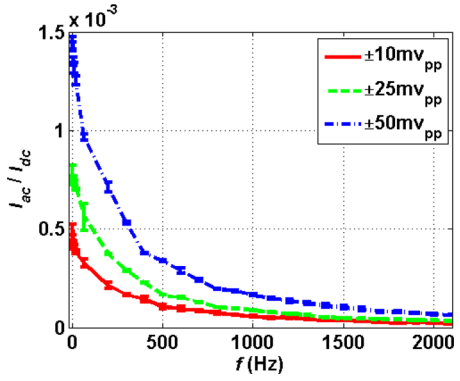

Figure 9. Frequency dependence of ac signal of 16 nm Au film.

capacitance of gold film, and the consequent scattering contrast and charging time. The importance of this investigation was that the 16 nm Au film retained its capability to response ±10 mV potential with frequency up to 2000 Hz. This would provide a potential route to optical detection of neural activity by using tunable noble metal nanoparticle based plasmonic sensor.

AUTHOR INFORMATION

Corresponding Author

*E-mail: huangyu@cigit.ac.cn.

Notes

The authors declare no competing financial interest.

ACKNOWLEDGMENTS

The authors gratefully acknowledge the financial support of the EPSRC (Grant No. EP/G005184/1), the UK.

REFERENCES

(1) Doron-Mor, I.; Barkay, Z.; Filip-Granit, N.; Vaskevich, A.; Rubinstein, I. *Chem. Mater.* **2004**, *16*, 3476.
(2) Xu, G.; Tazawa, M.; Jin, P.; Nakao, S *Appl. Phys. A: Mater. Sci. Process* **2005**, *80*, 1535.
(3) Huang, X. H.; Neretina, S.; El-Sayed, M. A. *Adv. Mater.* **2009**, *21*, 4880.
(4) Eustis, S.; El-Sayed, M. A. *Chem. Soc. Rev.* **2006**, *35*, 209.
(5) Toyota, A.; Nakashima, N.; Sagara, T. *J. Electroanal. Chem.* **2004**, *565*, 335.
(6) Ung, T.; Giersig, M.; Dunstan, D.; Mulvaney, P. *Langmuir* **1997**, *13*, 1773.
(7) Toyota, A.; Sagara, T. *Electrochim. Acta* **2008**, *53*, 2553.

(8) McIntyre, J. D. E. *Surf. Sci.* **1973**, *37*, 658.
(9) Novo, C.; Funston, A. M.; Gooding, A. K.; Mulvaney, P. *J. Am. Chem. Soc.* **2009**, *131*, 14664.
(10) Zhang, J. Y.; Atay, T.; Nurmikko, A. V. *Nano Lett.* **2009**, *9*, 519.
(11) Huang., Y.; Pitter, M. C.; Somekh, M. G *Langmuir* **2011**, *27*, 13950.
(12) Toyama, S.; Takei, O.; Tsuge, M.; Usami, R.; Horikoshi, K.; Kato, S. *Electrochem. Commun.* **2002**, *4*, 540.
(13) Panta, Y. M.; Liu, J.; Cheney, M. A.; Joo, S. W.; Qian, S. Z. *J. Colloid Interface Sci.* **2009**, *333*, 485.
(14) Zhang, N.; Schweiss, R.; Zong, Y.; Knoll, W. *Electrochim. Acta* **2007**, *52*, 2869.
(15) Garland, J. E.; Assiongbon, K. A.; Pettit, C. M.; Roy, D. *Anal. Chim. Acta* **2003**, *475*, 47.
(16) Sigel, J.; Lyutakov, O.; Rybka, V.; Kolska, Z.; Svorcik, V. *Nanoscale Res. Lett.* **2011**, *6*, 96.
(17) Liu, Z. H.; Brown, N. M. D.; McKinley, A. *J. Phys.: Condens. Matter.* **1997**, *9*, 59.
(18) Toyota, A.; Sagara, T. *Colloids Surf., A.* **2006**, *286*, 62.
(19) Jovic, V. D.; Jovic, B. M. *J. Electroanal. Chem.* **2003**, *541*, 13.
(20) Pajkossy, T.; Wandlowski, T.; Kolb, D. M. *J. Electroanal. Chem.* **1996**, *414*, 209.
(21) Pajkossy, T.; Kolb, D. M. *Electrochem. Commun.* **2007**, *9*, 1171.
(22) Kerner, Z.; Pajkossy, T. *Electrochim. Acta* **2000**, *46*, 207.